



OPEN ACCESS

EDITED BY

Xudong Zhu,
Xiamen University, China

REVIEWED BY

Xiaojuan Tong,
Beijing Forestry University, China
Chengcheng Gang,
Chinese Academy of Sciences (CAS), China

*CORRESPONDENCE

Fangjie Mao
✉ mfangjie@gmail.com

RECEIVED 21 December 2023

ACCEPTED 12 February 2024

PUBLISHED 26 February 2024

CITATION

Xu C, Mao F, Du H, Li X, Sun J, Ye F, Zheng Z,
Teng X and Yang N (2024) Full phenology
cycle carbon flux dynamics and driving
mechanism of Moso bamboo forest.
Front. Plant Sci. 15:1359265.
doi: 10.3389/fpls.2024.1359265

COPYRIGHT

© 2024 Xu, Mao, Du, Li, Sun, Ye, Zheng, Teng
and Yang. This is an open-access article
distributed under the terms of the [Creative
Commons Attribution License \(CC BY\)](#). The
use, distribution or reproduction in other
forums is permitted, provided the original
author(s) and the copyright owner(s) are
credited and that the original publication in
this journal is cited, in accordance with
accepted academic practice. No use,
distribution or reproduction is permitted
which does not comply with these terms.

Full phenology cycle carbon flux dynamics and driving mechanism of Moso bamboo forest

Cenheng Xu^{1,2,3}, Fangjie Mao^{1,2,3*}, Huaqiang Du^{1,2,3}, Xuejian Li^{1,2,3},
Jiaqian Sun^{1,2,3}, Fengfeng Ye^{1,2,3}, Zhaodong Zheng^{1,2,3},
Xianfeng Teng^{1,2,3} and Ningxin Yang^{1,2,3}

¹State Key Laboratory of Subtropical Silviculture, Zhejiang Agriculture and Forestry University, Lin'an, Zhejiang, China, ²Key Laboratory of Carbon Cycling in Forest Ecosystems and Carbon Sequestration of Zhejiang Province, Zhejiang Agriculture and Forestry University, Lin'an, Zhejiang, China, ³School of Environmental and Resources Science, Zhejiang Agriculture and Forestry University, Lin'an, Zhejiang, China

Introduction: Moso bamboo forests, widely distributed in subtropical regions, are increasingly valued for their strong carbon sequestration capacity. However, the carbon flux variations and the driving mechanisms of Moso bamboo forest ecosystems of each phenology period have not been adequately explained.

Methods: Hence, this study utilizes comprehensive observational data from a Moso bamboo forest eddy covariance observation for the full phenological cycle (2011–2015), fitting a light response equation to elucidate the evolving dynamics of carbon fluxes and photosynthetic characteristics throughout the entire phenological cycle, and employing correlation and path analysis to reveal the response mechanisms of carbon fluxes to both biotic and abiotic factors.

Results: The results showed that, First, the net ecosystem exchange (NEE) of Moso bamboo forest exhibits significant variations across six phenological periods, with LS_{OFF} demonstrating the highest NEE at $-23.85 \pm 12.61 \text{ gC}\cdot\text{m}^{-2}\cdot 5\text{day}^{-1}$, followed by LS_{ON} at $-19.04 \pm 11.77 \text{ gC}\cdot\text{m}^{-2}\cdot 5\text{day}^{-1}$ and FG_{ON} at $-17.30 \pm 9.58 \text{ gC}\cdot\text{m}^{-2}\cdot 5\text{day}^{-1}$, while NF_{OFF} have the lowest value with $3.37 \pm 8.24 \text{ gC}\cdot\text{m}^{-2}\cdot 5\text{day}^{-1}$. Second, the maximum net photosynthetic rate (P_{max}) and apparent quantum efficiency (α) fluctuated from 0.42 ± 0.20 (FG_{ON}) to $0.75 \pm 0.24 \text{ mg}\cdot\text{m}^{-2}\cdot\text{s}^{-1}$ (NF_{OFF}) and from 2.3 ± 1.3 (NF_{OFF}) to $3.3 \pm 1.8 \mu\text{g}\cdot\mu\text{mol}^{-1}$ (LS_{OFF}), respectively. Third, based on the path analysis, soil temperature was the most important driving factor of photosynthetic rate and NEE variation, with path coefficient 0.81 and 0.55, respectively, followed by leaf area index (LAI), air temperature, and vapor pressure difference, and precipitation. Finally, interannually, increased LAI demonstrated the potential to enhance the carbon sequestration capability of Moso bamboo forests, particularly in off-years, with the highest correlation coefficient with NEE (-0.59) among the six factors.

Discussion: The results provide a scientific basis for carbon sink assessment of Moso bamboo forests and provide a reference for developing Moso bamboo forest management strategies.

KEYWORDS

Moso bamboo forest, full phenology cycle, carbon flux, photosynthetic parameters, driving force analysis

1 Introduction

Forest carbon flux is a major component of the terrestrial ecosystem carbon cycle, accounting for over 90% of the total carbon exchanged between terrestrial ecosystems and the atmosphere (Friedlingstein et al., 2022), and plays an important role in maintaining regional ecological balance (Iturbide et al., 2020; Zhao et al., 2022). Forest carbon flux monitoring methods mainly include sample plot inventory, model simulation, and micrometeorological methods (Zhao et al., 2022). The sample inventory method is the most basic and accurate, but it comprises a large workload and is easily constrained by time and space. Model simulation includes statistical, parameter, and process-based models, which can provide support for studying forest ecosystem carbon cycling on a large scale, but due to spatiotemporal complexities and input parameter uncertainty, the simulation results of different models differ considerably (Mao et al., 2017a). The micrometeorological method usually refers to the eddy covariance CO₂ flux observation technique, the only method for directly determining the exchange of community CO₂ with the atmosphere that is widely used in global carbon flux observations (Gong et al., 2020). The flux observation networks, such as AmeriFlux, ChinaFlux, AsiaFlux and FLUXNET, provide important data for observing ecological phenomena from individual and community levels to the dynamic changes in ecosystem functions on a large scale. For example, Harris et al. (2021) used FLUXNET observations to map global forest carbon flux in the 21st century; Chu et al. (2021) evaluated flux footprints and the representativeness of these footprints for target areas by AmeriFlux; Chang et al. (2023) combined random forest with ChinaFlux data to estimate the GPP for the 9 sites. Therefore, the use of eddy covariance system to monitor the dynamics of regional carbon fluxes is an effective and currently well-respected approach.

Biotic and abiotic factors are important factors affecting carbon fluxes in forest ecosystems, and the extent and mechanisms of their effects are complicated by different vegetation physiological characteristics and growing environments (Baldocchi et al., 2018). For example, Xie et al. (2014) found that an increase in temperature reduces carbon sequestration by increasing respiration, but Richardson et al. (2010) pointed out that warming in a certain range increases photosynthesis, which increases ecosystem carbon sequestration. Regardless, it has become a scholarly consensus that ecosystem respiration, a major factor in carbon emissions, is primarily influenced by temperature, especially in moisture-rich regions (Kondo et al., 2017). However, besides abiotic factors such as temperature and radiation, vegetation photosynthesis is also influenced by growth cycles (phenology) and canopy structure (e.g., leaf area index [LAI]) (Gitelson et al., 2017). Therefore, analyzing the characteristics of photosynthetic carbon fixation and elucidating the effect of photosynthesis on carbon fluxes is a hotspot in studying the mechanism of carbon fluxes influence in forest ecosystems. Fitting the light response equations of different vegetation is an important method for understanding dynamic plant physiology processes (Zhang et al., 2006; Li et al., 2014; Zhou et al., 2017). Apparent quantum efficiency (α) and maximum photosynthetic rate (P_{max}) are important characteristic

parameters in the vegetation light response equation, which can accurately describe the characteristics of vegetation photosynthesis and its intensity (Lin et al., 2022).

Subtropical forest ecosystems in the East Asian monsoon zone has a non-negligible role in mitigating global warming, and its net ecosystem productivity is 0.72 Pg C·a⁻¹ (Yu et al., 2014). Moso bamboo (*Phyllostachys edulis*) is a special forest type widely distributed in subtropical areas, with an annual NEE approximately of -105.2 gC·m⁻²·a⁻¹, indicating a strong pathway model carbon sequestration potential for mitigating climate change (Song et al., 2020). However, Moso bamboo has special phenological and growth characteristics, i.e., the alternation of on- and off-years (mass of bamboo shoots in one year, and almost none in another), and “explosive growth” of new bamboo (Mao et al., 2017a). Several studies explored the spatiotemporal patterns of carbon storage, productivity and carbon fluxes and their response to climate change (Mao et al., 2022; Yan et al., 2023), such as Mao et al. (Mao et al., 2016; Mao et al., 2017a) adapted the BIOME-BGC model for the simulation of managed Moso bamboo forest ecosystems, and simulated the carbon fluxes of bamboo forests in Zhejiang Province, China (Mao et al., 2017b); Kang et al. (2022) used the BEPS model to simulate the carbon fluxes of bamboo forests in China; Li et al. (2021) estimated GPP of subtropical bamboo forests by assimilated-LAI. In addition, the start and length of the growing season of subtropical bamboo forest had been successfully retrieved using LAI and SIF datasets (Li et al., 2023; Xu et al., 2023). However, the key drivers under different time scalars are still unclear, such as Liu et al. (2018) found the most important factor affecting net ecosystem change (NEE) and respiration (RE) at daily scalar was vapor pressure difference (VPD), while at monthly scalar was soil temperature (Ts). Zhou et al. (2019) indicated that the effect of biotic and abiotic factors differs in on- and off-years. Moreover, lacks of the carbon flux dynamics and driving mechanism throughout the whole phenology cycle of Moso bamboo forests, bring huge uncertainties in accurately assessing the response of bamboo forests to climate change at a large spatial scale (Huang et al., 2023; Xu et al., 2023; Yan et al., 2023).

Therefore, this study obtained and correlated the carbon fluxes, biotic and abiotic factors of full phenology cycle of Moso bamboo forests based on the eddy covariance observation from 2011 to 2015, analyzed the dynamic and differences of carbon fluxes and photosynthetic indices during six Moso bamboo specific phenology period, and finally quantitatively analyzed the direct and indirect effects of abiotic and biotic factors on carbon fluxes using the combination of correlation and path analysis methods.

2 Materials and methods

2.1 Study area

The Moso bamboo forest ecosystem flux observation station (Figures 1A, B) is located in Anji County, Zhejiang Province, China (30.46°N, 119.66°E). The forest area is 13.8 × 10⁴ hm², the forest coverage rate is 71% in Anji. The climate type is subtropical

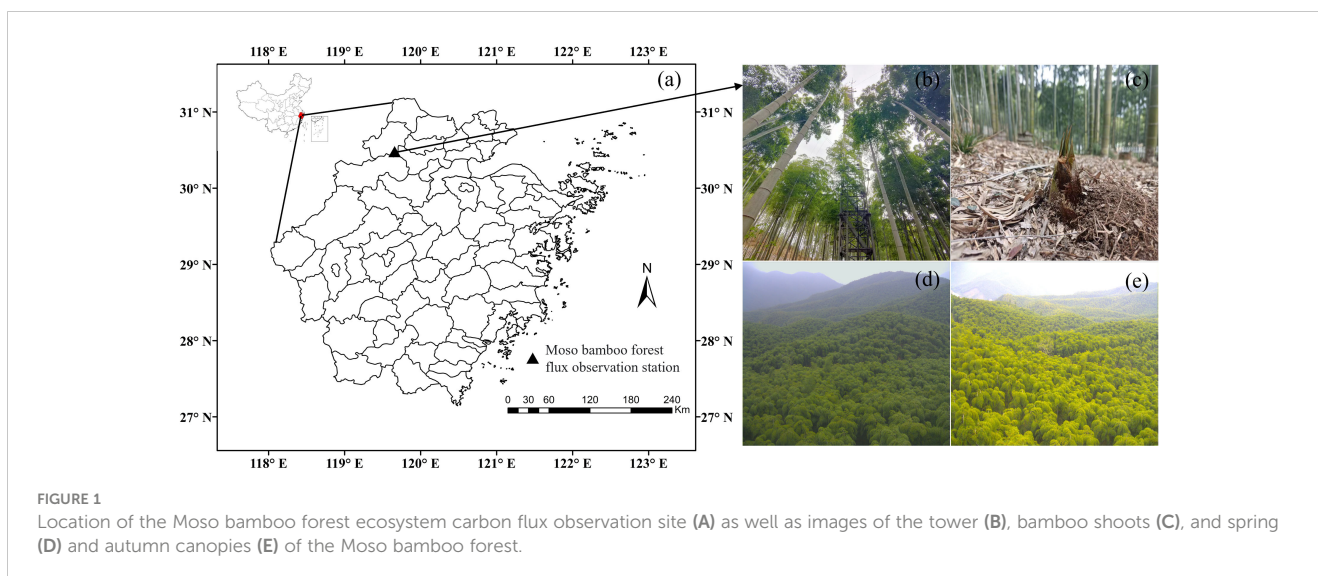


FIGURE 1

Location of the Moso bamboo forest ecosystem carbon flux observation site (A) as well as images of the tower (B), bamboo shoots (C), and spring (D) and autumn canopies (E) of the Moso bamboo forest.

monsoon, the average annual temperature is 16.6 °C, the average annual precipitation is 1400 mm, and the annual sunshine hours are 2021 h. The altitude of the flux observation station is 380 m, the terrain is flat in the southeastern and southern parts of the observation tower, and the slope in the northwestern and northern parts of the observation tower ranges from 2.5° to 14°, and the Moso bamboo forest is dominant within 1 km × 1 km of the observation tower. The area of Moso bamboo forest is 2155 hm², with an average crown height of 11 m, an average diameter at breast height of 9.3 cm, and yellow loam and yellow-red loam soil types, with sparse herbs and shrubs in the understory, which are pure Moso bamboo forests operated by artificial rough management (Liu et al., 2018). The growth cycle of Moso bamboo forests comprises a 2-year cycle, with a first year, known as on-year, comprising a large number of shoots, and a second year, known as off-year, comprising a small number of shoots, in which the growth period is generally concentrated in March–September (Li et al., 2019).

2.2 Sample survey

2.2.1 Carbon fluxes and micrometeorological data in Moso bamboo forest ecosystems

Carbon fluxes and micrometeorological data were obtained by 40 m high flux tower equipped with open-path eddy-covariance system (OPEC), atmospheric profile system (APS), and gradient micrometeorological system (GMS). The OPEC was deployed at 38 m according to the height of the forest stand canopy, while the APS and GMS were deployed at seven levels (1, 7, 11, 17, 23, 30, and 38 m) on both sides of the tower arm. The OPEC comprised a 3-D sonic anemometer (CSAT3, Campbell Scientific, USA) and an open-path CO₂/H₂O analyzer (Li-7500, Li-COR Biosciences, USA). The APS was deployed to obtain real-time CO₂ and H₂O concentration by AP200 (Campbell Scientific, USA). The GMS included temperature and humidity sensor (HMP155, Vaisala, Finland), wind speed sensor (WindSonic, Gill Instruments, UK), 4-component net radiometer (CNR4, Campbell Scientific, USA),

soil moisture and temperature profile sensor (SoilVUE10, Campbell Scientific, USA) and soil heat flux sensor (HFP01, Hukseflux, Netherlands) at depths of 5, 10, 20, 30, 40 and 50 cm. Systematic observation data, including physical quantities such as CO₂ flux at 10 Hz, friction wind speed, and other relevant physical quantities, as well as 30-min averaged conventional meteorological information, were stored using a CR1000 data collector (Campbell Scientific, USA).

2.2.2 LAI data

LAI was based on sample LAI combined with MODIS LAI and reflectance to assimilate an LAI time series. The sample LAI was determined using a WinSCANOPY canopy analysis system (Regent Instruments, Canada). The specific method included setting up five fixed sample points within 1000 m from the flux tower as the center. To ensure LAI measurement accuracy and avoid light spot formation on the image due to solar radiation, measurement was conducted at 6:00–10:00 and 15:00–17:50 monthly, when it was sunny, without cumulus clouds, and with good atmosphere visibility. Canopy images were obtained using the fisheye lens that came with the canopy analyzer, brought back to the laboratory, and post-processed using the corresponding software. The average of five sample points was taken as the LAI measurement in the field.

The MODIS LAI data assimilation system mainly used the particle filter assimilation algorithm to assimilate MODIS LAI, reflectance data, and PROSAIL model-simulated canopy reflectance into the LAI dynamic model to obtain a high-precision bamboo forest LAI time series product (Fang et al., 2003; Li et al., 2017).

2.2.3 Observation of Moso bamboo phenology

For the purpose of economic beneficial, the farmers usually harvested nearly all Moso bamboo of six years or older in the autumn, leading to a completely renewal of the bamboo stand every five years. This renewal cycle forms the basis of the full phenological cycle studied here. The Moso bamboo phenological observation including bamboo shooting, explosive growth, leaf spreading, and

leaf renewing (Figures 1C-E) during 2011 - 2015 using a camera deployed on 25 m of the tower, and the lens faces south with an inclination of 20° (Xu et al., 2023). In this study, 2011, 2013 and 2015 belong to on-years, and others were off-years. Combined the phenological characteristics and on- (off-) year phenomena, the full phenology cycle was divided into six periods, and determined the start and end dates of each phenological period by phenology camera observations. The six periods are as follows: (1) fast-growing period (FG_{ON}), which refers to the stage when freshly sprouted culms grow above the ground and accomplish their height growth; (2) leaf-spreading in on-years (LS_{ON}), indicating the stage when freshly sprouted bamboo culms start flushing leaves; (3) leaf-renewing period (LR_{OFF}), describing the stage odd-year-old established culms shed old leaves and flush new leaves; (4) leaf-spreading in off-years (LS_{OFF}), which pertains to the stage new leaves are expanding on the odd-year-old established culms; (5, 6) other normal days in on- and off-years (NF_{ON} and NF_{OFF}). For the details of each phenology period, please refer to Mei et al. (2020).

2.3 Data processing

2.3.1 Half-hourly and daily carbon flux data acquisition

Carbon flux observation was made at the stand canopy level, raw data were processed to daily NEE, RE, and gross ecosystem productivity (GEP) (Mao et al., 2017a). Raw flux data were corrected using EddyPro v.6.0.0 (LI-COR Inc., USA) by spike removal, tilt correction (double-axis rotation), spectral correction, block averaging, correction for density fluctuations, and subsequent flux calculation (Baldocchi et al., 2018). When atmospheric turbulence is insufficient at night, soil and plant respiration are deposited below the forest canopy, which can easily lead to nighttime flux underestimation; therefore, a friction wind speed rejection threshold of 0.2 m·s⁻¹ (Xu et al., 2016a) was adopted in this study.

The steps for missing data interpolation were as follows: first, meteorological data with missing time ≤ 2 h and > 2 h were interpolated using linear interpolation and mean daily variation methods, respectively (Falge et al., 2001); second, the Lloyd-Taylor equation was used to fit the missing RE, by the way, since there is no photosynthesis at night so RE = NEE at night (Lloyd and Taylor, 1994); lastly, the right-angled hyperbolic equation was interpolated to the daytime NEE (Falge et al., 2001) to obtain the complete half-hourly carbon flux time series. On this basis, daily scale carbon fluxes were obtained by accumulation, and GEP calculated by RE minus NEE. In this study negative value of carbon fluxes indicate carbon sink, while positive refers to carbon source.

2.3.2 Extraction of photosynthetic parameters

The daytime 30-min flux samples were too small to fit photosynthetic parameters on a daily scale. Therefore, the apparent quantum efficiency (α , mg· μ mol⁻¹·s⁻¹) and maximum photosynthetic rate (P_{max} , mg·m⁻²·s⁻¹) were fitted using daytime NEE, RE, and PAR data in a 5-day window using the right-angle

hyperbolic equation (Equation 1) (Falge et al., 2001). Meanwhile, due to the high frequency of noise fluctuation in the fitting results, α and P_{max} were smoothed by Gaussian filter to show the trend of changes (Savitzky and Golay, 1964) of 73 values per year, matching the time series of the flux data.

$$-NEE = \frac{\alpha \times PAR \times P_{max}}{\alpha \times PAR + P_{max}} - RE \quad (1)$$

2.4 Data analysis

Correlation and path analysis methods were used to analyze the influence mechanisms of biotic and abiotic factors on carbon fluxes and photosynthetic parameters in a full phenological cycle of Moso bamboo forests.

Based on the above data, the time series of carbon fluxes, photosynthetic parameters, and abiotic factors in different phenological periods of Moso bamboo forest ecosystems from 2011 to 2015 were obtained. Subsequently, the correlation among indicators in different phenological periods was evaluated by using Pearson's correlation coefficient (r_{xy}), after which the path coefficient (PC) among indicators was calculated using the pathway model to analyze the direct and indirect impacts of the indicators on carbon fluxes and reveal the degree of influence of each factor on carbon fluxes, and then derive the changes in and driving mechanisms of carbon fluxes and photosynthetic parameters. r_{xy} was calculated using Equation 2:

$$r_{xy} = \frac{\sum_{i=1}^n (x_i - \bar{x})(y_i - \bar{y})}{\sqrt{\sum_{i=1}^n (x_i - \bar{x})^2 \sum_{i=1}^n (y_i - \bar{y})^2}} \quad (2)$$

where, x_i is the value of the six biotic and abiotic factors on day i , y_i represents the three carbon flux values as well as the two photosynthetic parameters, \bar{x} and \bar{y} represent the total mean values of the biotic and abiotic factors with respect to carbon fluxes and photosynthetic parameters, respectively, n is the total number of days, and i denotes ordinal days ($i = 1, 2, \dots, n$).

Path analysis was conducted using SPSSPRO Ver.1.0.11 (<https://www.spsspro.com>). NEE was determined using GEP and RE; GEP is directly affected by the photosynthesis (Chen et al., 2009), while P_{max} is important in determining the photosynthetic capacity of ecosystems (Zhang et al., 2006; Flexas and Carriqui, 2020). Based on this logic, the structure of the pathway model constructed in this study is shown in Figure 2.

3 Results

3.1 Characteristics of biotic and abiotic factor changes in Moso bamboo forests

As shown in Figure 3, VPD, precipitation (Prec), PAR, LAI, T_a , and T_s had significant seasonal characteristics, with higher values in summer. VPD fluctuated more, especially in 2013 and 2015, the

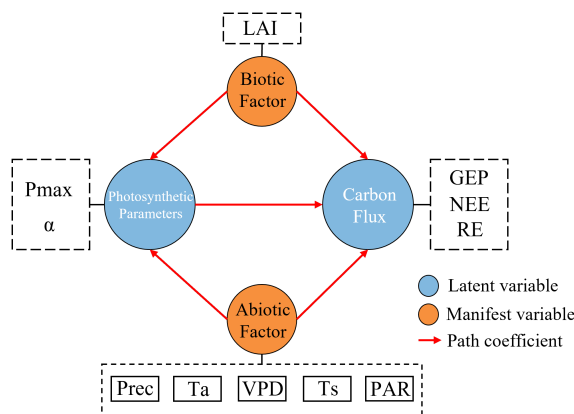


FIGURE 2
Structure of the inter-variable pathway. VPD, vapor pressure difference; Prec, precipitation; PAR, photosynthetic radiation; LAI, leaf area index; Ta, air temperature; Ts, soil temperature.

difference between their maximum and minimum values are 28.93 kPa and 23.11 kPa, respectively, and relatively less in 2011(16.55 kPa), 2012(16.02 kPa) and 2014(13.82 kPa).

The highest annual mean temperature was 15.3°C in 2013, the lowest was 14.1°C in 2014, the highest annual precipitation was 2143 mm in 2012, and the lowest was 1363 mm in 2014. PAR annual average was highest in 2013(260.50 μmol·m⁻²·s⁻¹) and lowest in 2015(197.70 μmol·m⁻²·s⁻¹). The annual mean values of LAI were 4.02, 4.46, 4.17, 4.34, and 3.78 from 2011 to 2015, respectively. The mean LAI was higher in the off-years (4.40) than that in the on-years (3.99), and the interannual maximum LAI was in summer (2011-2013) or autumn (2014-2015).

3.2 Comparison of carbon fluxes and photosynthetic parameters across the full phenological cycle

As shown in Figures 4A–C, NEE and GEP showed a bimodal pattern in the on-years, with the two peaks occurring in FG_{ON} and LS_{ON}, respectively, and in the same period in the off-years, they occurred in LR_{OFF} and LS_{OFF}, respectively. The changes in RE exhibited similar trends between on- and off-years. GEP averaged 2871.40 gC·m⁻²·a⁻¹ in the on-years, with an average maximum of 82.13 gC·m⁻² in summer and an average minimum of 9.87 gC·m⁻² in winter, while in the off-years it averaged 2829.49 gC·m⁻²·a⁻¹, with an average maximum of 75.08 gC·m⁻² in summer and an average minimum of 6.17 gC·m⁻² in winter. NEE averaged -1071.99 gC·m⁻²·a⁻¹ in the on-years, with a mean maximum of 11.08 gC·m⁻² and a minimum of -42.46 gC·m⁻², and -1051.70 gC·m⁻²·a⁻¹ in the off-years, with a mean maximum of 16.99 gC·m⁻² and a mean minimum of -47.81 gC·m⁻². The RE in the on-years averaged 1799.41 gC·m⁻²·a⁻¹, with a mean maximum of 41.68 gC·m⁻² and a mean low point of 10.29 gC·m⁻², and the off-years averaged 1777.79 gC·m⁻²·a⁻¹, with a mean maximum of 39.99 gC·m⁻² and minimum of 4.64 gC·m⁻².

As shown in Figures 4D–F, the mean values of carbon fluxes in six different phenological periods of the on- and off-years were determined

according to the on- and off-year time series, starting from FG_{ON} to NF_{ON} as a growth cycle. The mean value of NEE in FG_{ON} was -17.30 ± 9.58 gC·m⁻², and that in LR_{OFF} was -11.75 ± 12.77 gC·m⁻²; the absolute value of NEE in FG_{ON} was higher than that of LR_{OFF}. The mean value of NEE in LS_{ON} was -19.04 ± 11.77 gC·m⁻², lower than that of NEE in LS_{OFF} at 23.85 ± 12.61 gC·m⁻². NF_{OFF} had an NEE of -3.37 ± 8.24 gC·m⁻², while NF_{ON} had an NEE of -12.19 ± 11.42 gC·m⁻². RE was highest for LS_{ON} at 29.08 ± 4.90 gC·m⁻²; similar for FG_{ON}, LR_{OFF}, and LS_{OFF} at 26.24 ± 4.04, 26.53 ± 6.32, and 26.39 ± 6.55 gC·m⁻², respectively, and lower for NF_{OFF} and NF_{ON} at 22.01 ± 4.45 and 21.48 ± 4.82 gC·m⁻², respectively. GEP was highest in the leaf spreading period, with LS_{ON} and LS_{OFF} at 48.12 ± 12.84 and 50.24 ± 16.15 gC·m⁻², respectively. FG_{ON} had greater GEP than that of LR_{OFF} (43.54 ± 8.65 vs. 38.28 ± 13.24 gC·m⁻²), whereas NF_{OFF} had the lowest at 25.38 ± 8.56 gC·m⁻², and NF_{ON} had a slightly higher GEP than that of the NF_{OFF} at 34.12 ± 12.36 gC·m⁻².

As shown in Figure 5B, P_{max} and α showed a significant negative correlation (P < 0.05), and the trend of α in an operating cycle was roughly opposite to that of P_{max}. As shown in Figure 5A, the mean P_{max} value in the on-years (2011, 2013, and 2015) was 0.64 mg·m⁻²·s⁻¹ and showed a bimodal pattern of change, with a mean value of α of 2.95 μg·μmol⁻¹. The mean P_{max} value in the off-years (2012 and 2014) was 0.58 mg·m⁻²·s⁻¹ and exhibited a single-peak pattern of change, with a mean α of 2.90 μg·μmol⁻¹. The P_{max} peak in 2013 was substantially lower than that in 2011 and 2015. The first P_{max} peak in the on-years occurred at FG_{ON}, and the second occurred at the end of LS_{ON}; the P_{max} peak in off-years occurred at LS_{OFF}.

As shown in Figure 6A, the highest mean P_{max} value was 0.75 ± 0.24 mg·m⁻²·s⁻¹ in LS_{OFF}, and the lowest was 0.42 ± 0.20 mg·m⁻²·s⁻¹ in NF_{ON}, while the highest and lowest values for both on- and off-years corresponded to the LS and NF periods, similar to GEP. As shown in Figure 6B, the maximum value of α appeared at NF_{ON}, and the minimum value was at NF_{ON}. According to the quartiles, the distribution of P_{max} was more concentrated in LS_{ON} and more homogeneous in LR_{OFF}. The distribution of α is more discrete relative to that of P_{max}.

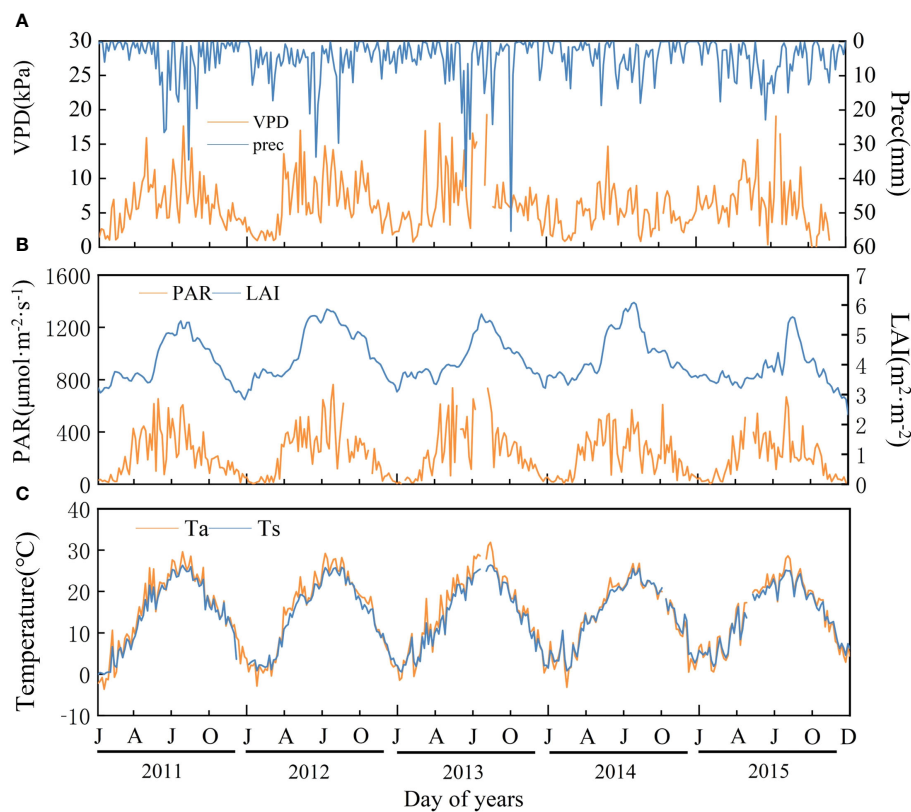


FIGURE 3 Variation in biotic and abiotic factors of Moso bamboo forests during 2011–2015. (A) VPD (vapor pressure difference) and Prec (precipitation); (B) PAR (photosynthetic radiation) and LAI (leaf area index); (C) Ta, (air temperature) and Ts (soil temperature). Interruptions are missing data.

3.3 Analysis of the drivers of carbon flux throughout the full phenological cycle

As shown in Figure 7, carbon fluxes during the six phenological periods were most closely correlated with temperature, and the correlation with Ts was higher than that with Ta, with the highest correlation in FG_{ON} and the lowest in LR_{OFF} and LS_{OFF}. Of the three carbon fluxes, the correlation with temperature varied considerably during the early, middle, and last part of each year. The highest correlation between temperature and NEE was observed in FG_{ON} and LR_{OFF}, with Ts and Ta being highly significantly correlated with NEE in the FG_{ON} stage (0.26 and 0.31, $P < 0.01$, respectively) but not in LR_{OFF}. The highest correlation with RE was in NF_{ON} (Ts: 0.36, $P < 0.01$; Ta: 0.27, $P < 0.05$) and NF_{OFF} (Ts: 0.40, $P < 0.01$; Ta: 0.39, $P < 0.01$). The highest correlation with GEP was in the LS_{ON} (Ts: -0.42, $P < 0.05$; Ta: -0.32) and LS_{OFF} periods (Ts: 0.25, $P < 0.05$; Ta: 0.21). Moisture factors (Prec and VPD) correlated with carbon fluxes to a lesser extent than temperature, which was significant at LS_{OFF} and NF_{ON} (LS_{OFF}: Prec, and VPD to RE: 0.27, $P < 0.05$ and -0.27, $P < 0.05$, respectively; NF_{ON}: Prec to NEE and GEP: 0.29, $P < 0.05$ and -0.25, $P < 0.05$, respectively, and VPD to NEE and GEP: -0.32, $P < 0.01$ and 0.28, $P < 0.05$, respectively). Meanwhile, the correlation of moisture factors with carbon fluxes in the early, middle, and last stages of the year showed a different pattern from that of temperature, with

the highest correlation being with respiration in all remaining periods except for NF_{OFF}, which was the lowest. The correlation between PAR and carbon fluxes was mainly with NEE (negative) and GEP (positive) and was dominated by significant correlations between LS_{OFF} and NF_{ON} (-0.25, $P < 0.05$ for PAR to NEE in LS_{OFF}; -0.46, $P < 0.01$ and 0.45 for PAR to NEE and GEP in NF_{ON}, $P < 0.01$). The response of carbon fluxes to LAI was mainly in NF_{OFF}, with correlations of 0.40 ($P < 0.01$) and 0.28 ($P < 0.01$) with RE and GEP, respectively, and LS_{OFF}, with a correlation of -0.45 ($P < 0.05$) with NEE. Interannually, the six factors were significantly correlated with carbon fluxes, with Ts being the most highly significant and Prec the lowest.

For photosynthetic parameters of Figure 7, the correlation with temperature was high in the stem growth stage (FG_{ON}), with water in the LS, and the effect of PAR was mainly seen after leaf formation (LS, NF). Interannually, the correlation of LAI with photosynthetic parameters was higher in the off-years (LAI to P_{max} and α were 0.52, $P < 0.01$ and -0.19, $P < 0.05$, respectively) than that in on-years (LAI to P_{max} and α were 0.07 and -0.01, respectively), with the former being significant and the latter not. Meanwhile, similar to carbon fluxes, both had temperature as the most significant driver.

The path analysis results of biotic and abiotic factors on carbon fluxes during different phenological periods are shown in Figure 8, and the complete PCs are shown in Appendix A. Figure 8 shows that Ta, Ts, and LAI were the most influential factors on the P_{max} of

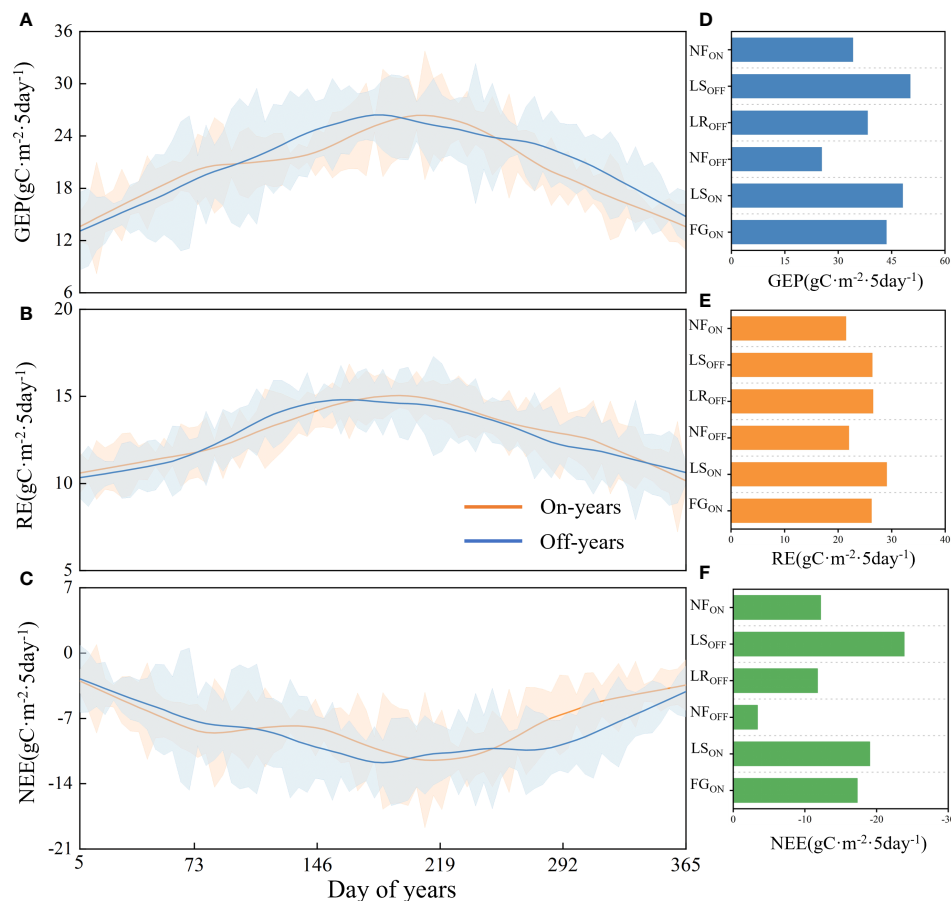


FIGURE 4 Carbon fluxes in on- and off-years in Moso bamboo forests (A–C) and corresponding statistic by every phenological period (D–F). Solid lines are filtered trend lines. Blue shading is standard deviation of off-years, orange is of on-years.

Moso bamboo, where Ta acted as a facilitator in FG_{ON} and NF_{ON} ($\text{PC} = 1.12$ and 0.73 , respectively), and an inhibitor in LR_{OFF} , LS_{ON} , and LS_{OFF} ($\text{PC} = -0.91$, -0.52 , and -1.35 , respectively). Ts acted as a facilitator in LS_{ON} , LS_{OFF} , and NF_{OFF} ($\text{PC} = 0.49$, 1.38 , and 0.56 , respectively) and an inhibitor in FG_{ON} and NF_{ON} ($\text{PC} = -1.41$ and -0.62). LAI acted as a facilitator and inhibitor in LR_{OFF} ($\text{PC} = 0.67$) and NF_{OFF} ($\text{PC} = -0.40$), respectively. The direct effect of P_{max} on GEP was mainly as a facilitator, with PCs ranging from 0.17 to 0.85

(Supplementary Figure S1), whereas the indirect effect of the biotic and abiotic factors on GEP was mainly realized through P_{max} , whose effect on P_{max} was similar. On an interannual scale, Ts dominated the increasing effects of P_{max} and GEP in both on- and off-years (mean $\text{PC} = 3.48$ and 1.94 , respectively), and Ta acted as a suppressor (mean $\text{PC} = -1.27$ and -0.96 , respectively).

Overall, all factors except Prec dominated the carbon sink (NEE reduction) at different stages; FG_{ON} , LR_{OFF} , LS_{ON} , LS_{OFF} , NF_{ON} ,

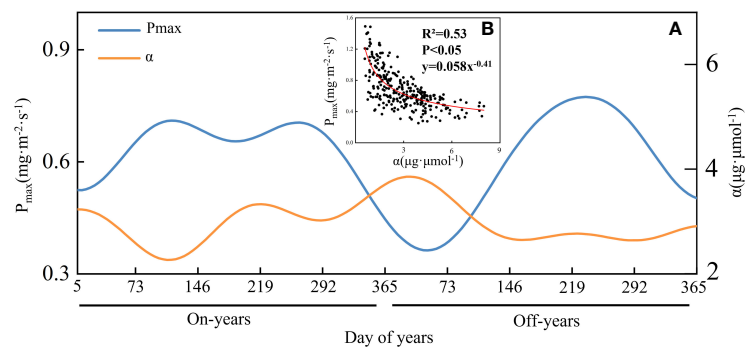


FIGURE 5 The time series of P_{max} and α in Moso bamboo forests (A), as well as their scatterplots (B) and allometric fitting curve (red).

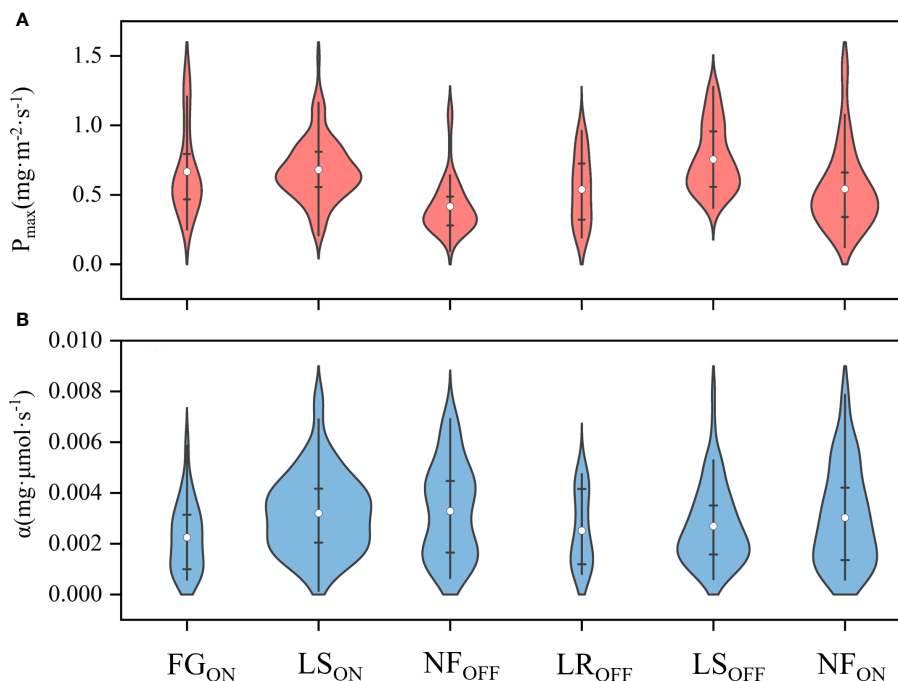


FIGURE 6 Violin plots of average photosynthetic parameters of P_{max} (A) and α (B) in Moso bamboo forests. White dots are mean values.

and NF_{OFF} were dominated by Ta (PC = -0.54), LAI (PC=-0.36), PAR (PC = -0.10), Ts (PC = - 1.42), Ta (PC = -0.54), and VPD (PC = -0.26). The dominant factors that contributed to the carbon source (NEE increase) in Moso bamboo forests were Ts and Ta, where Ts was mainly in FG_{ON} (PC = 0.88) and NF_{ON} (PC = 0.65), and Ta was in LR_{OFF} (PC = 0.32), LS_{ON} (PC = 0.23), LS_{OFF} (PC = 1.63), and NF_{OFF} (PC = 0.39). From the interannual results, Ts was overall the most dominant driver of the increase in carbon sinks in both on- and off-years, with a PC of -0.08 in on-years and -1.35 in off-years. The factors that contributed most to the increase in NEE were LAI and Ta in on- and off-years, with PCs of 0.23 and 1.27, respectively.

4 Discussion

4.1 Carbon fluxes and photosynthetic parameters of full phenological cycle

Although similar environmental elements are present in FG_{ON} and LR_{OFF}, the absolute values of NEE and GEP are higher in FG_{ON} than in LR_{OFF}, probably due to more carbon fixed in a short period by the “explosive growth” of the on-years (Song et al., 2016). In contrast, the LR_{OFF} stage consisted of leaf replacement during the same period, resulting in an overall lower photosynthetic capacity than that of the former (Gu et al., 2019). Therefore, a significant difference could be seen in carbon fluxes between the two periods. Furthermore, based on the fact that photosynthetic parameters can somewhat reflect the magnitude of photosynthetic capacity (Lin et al., 2022), the average P_{max} of FG_{ON} was not only higher than that

of LR_{OFF} but also higher than that of the previous phenological period (NF_{OFF}), suggesting that high carbon sequestration rates during the “explosive growth” period may be due to the rapidly increasing photosynthetic capacity (Song et al., 2017), which also contributed to the bimodal NEE trend. We also noticed a decreasing NEE trend in June, which may be due to the high rainfall during the rainy season, which reduces photosynthesis on the one hand and increases soil respiration on the other hand, thus leading to decreased NEE (Chen et al., 2016). Moreover, anthropogenic factors also somewhat affected the carbon flux of the Moso bamboo forest ecosystem, mainly manifested in the lower absolute values of NEE and GEP in LS_{ON} than those in LS_{OFF}, primarily due to the decreased LAI caused by the selection and hooking of old bamboo in the current year, which led to decreased photosynthesis (Zheng et al., 2022). The RE of the full phenological cycle of Moso bamboo forests is similar to that of other forests and is also mainly influenced by temperature (Ge et al., 2020). We noted the proximity of RE and LR_{OFF} in FG_{ON} and the high transpiration in both periods (Gu et al., 2019), which may provide evidence for further arguments on the “explosive growth” of new Moso bamboo and the similar amount of nutrients utilized for leaf replacement in old bamboo.

From the photosynthetic pattern of Moso bamboo forests in on- and off-years, the average P_{max} of on-years is higher than that of off-years, and the average GEP is also slightly higher than that of off-years. P_{max} may be an important reason for the difference in the GEP of Moso bamboo forest ecosystems, and simultaneously, the changing pattern of GEP also verifies the previous sample plot scale observation experiment results (Zhang et al., 2011; Xu et al., 2016b). We also observed that P_{max} and α negatively correlated in Moso

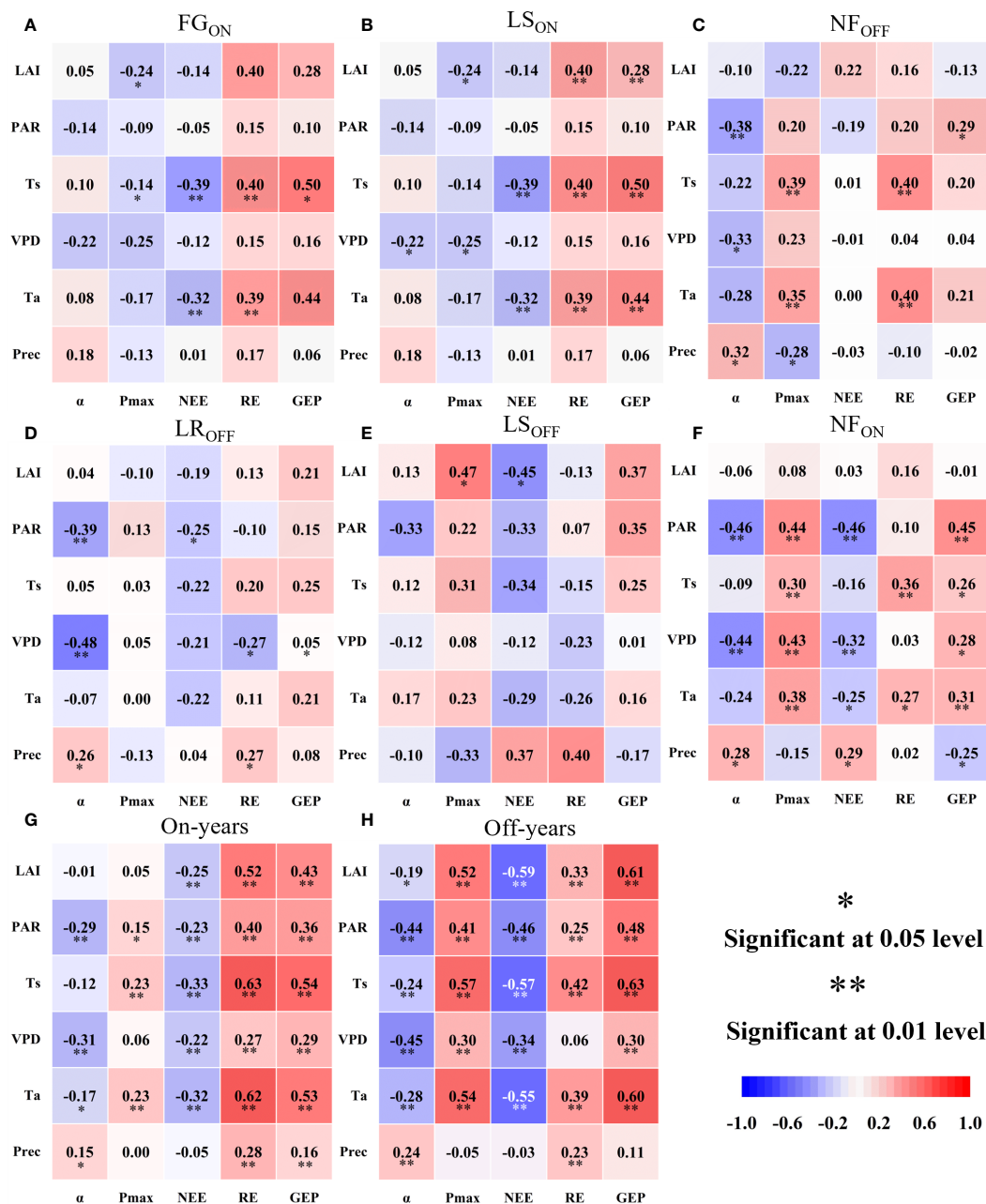


FIGURE 7 Pearson's correlation analysis of photosynthetic parameters and carbon fluxes with six biotic and abiotic factors over the full phenological cycle (A–F) and on-and off-years (G, H) of Moso bamboo forests.

bamboo forest ecosystems, while other subtropical forests usually show positive correlations (Lin et al., 2022; You et al., 2022), the reasons for which need to be further investigated in depth.

4.2 Carbon fluxes and photosynthetic parameters in response to biotic and abiotic factors

Based on six factors acting on NEE through P_{max} and through RE (Appendix A), we obtained the direct effects of biotic and abiotic

factors on P_{max} and RE as well as their indirect effects on NEE. Firstly, according to the pathway of “factors - P_{max} - GEP - NEE”. Ta, Ts, and LAI had the most direct impact on P_{max}, with Ts dominating in LS_{ON}, LS_{OFF}, and NF_{OFF} (Figures 8B, C, F), Ta dominating in FG_{ON} and NF_{ON} (Figures 8A, G), and LAI dominating in LR_{OFF} (Figure 8E). NEE pathway showed different indirect impacts by biotic and abiotic factors, in FG_{ON} and LR_{OFF}, the factor with the strongest promotion of P_{max} played a dominant role in the increase in sinks (NEE reduction) in Moso bamboo forest ecosystems (Figures 8A, E). However, from the pathway of “factors - RE - NEE”. We can see the same factors that dominated RE

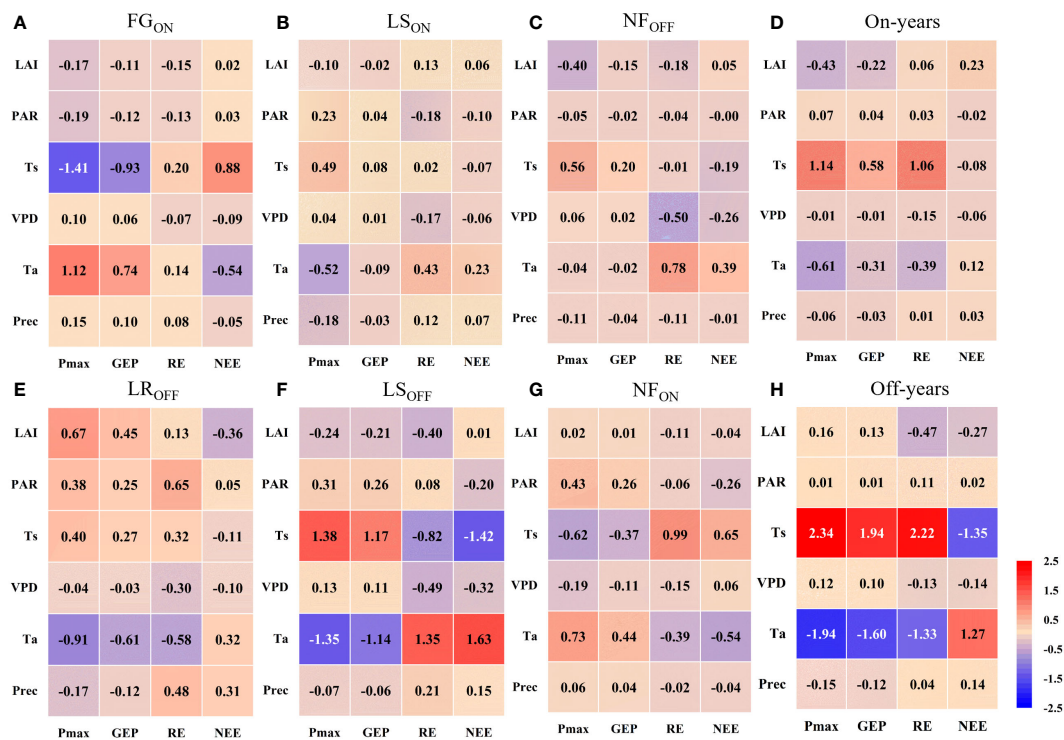


FIGURE 8 Path coefficients among factors in the full phenological periods (A–C, E–G) and on-and off- years (D, H) in Moso bamboo forests.

suppression during the LS_{ON}, LS_{OFF}, NF_{ON}, and NF_{OFF} periods also dominated sink enhancement (NEE increase) in Moso bamboo forest ecosystems (Figures 8B, C, F, G). The indirect effects of these two pathways on NEE suggesting that the photosynthetic capacity of Moso bamboo forest ecosystems plays a dominant role in increasing sinks when new bamboo grows explosively and old bamboo changes its leaves. This may be because the most important feature of FG_{ON} and LR_{OFF} lies in leaf change, which overshadows respiration in the change in photosynthetic capacity (Song et al., 2016; Mei et al., 2020) and further explains the important role of LAI in increasing carbon sinks by increasing photosynthesis (Gitelson et al., 2017). Contrastingly, in the remaining four periods, larger respiration was the main cause of lower carbon sinks.

Although RE played a dominant role in changes in NEE, except VPD in off-years, we found significant positive correlations ($P < 0.01$) between RE and the factors under interannual variation (Figures 7G, H). It revealed that respiration is overly sensitive to environmental responses, especially temperature factors (Ta and Ts). Meanwhile, respiration during LS periods were subject to a combination of water and heat (Figures 7B, E), which may be due to LS periods were the longest stage of six full phenological periods occurring in the in the summer and early autumn, with the presence of extreme climatic factors such as high/low temperatures, droughts and heavy precipitation (Du et al., 2020; Jia et al., 2020).

Both correlation and path analysis showed that temperature had the most important effect on NEE and RE in Moso bamboo forest ecosystems, but Ta and Ts acted in different directions, Ts focuses

on the effects on soil, root, and biological respiration in the belowground portion of the body (Tang et al., 2015; Jiang et al., 2016; Ge et al., 2020), whereas Ta focuses on aboveground respiration in the stem and leaf biomass (Wang et al., 2021). In addition, the interannual PC of Ts to RE was higher than that of Ta (Figures 8D, H), indicating that the subsurface fraction contributes more to respiration, and thus, reducing soil respiration has the most pronounced effect on sink enhancement (Luo and Zhou, 2010; Oikawa et al., 2017).

Comparatively, water factors (VPD, Prec) and PAR drove carbon fluxes much less than did temperature, with VPD showing a dominant role in respiratory inhibition only during the NF_{OFF} phase (Figure 8C), which may indicate that elevated VPD in winter may disrupt plant epidermal stomata (Hsu et al., 2021). PAR is intrinsically unrelated to the maximum photosynthetic capacity of the plant (Lin et al., 2022) and has a relatively low impact on respiration (Liu et al., 2018). However, it regulates GEP primarily by affecting real-time photosynthesis in Moso bamboo forests (Xu et al., 2016b).

Both correlation and path analysis showed that the six biotic and abiotic factors selected in the current study strongly correlated with carbon fluxes changes in Moso bamboo forests (Figures 7, 8). However, the correlations and the mechanisms of direct and indirect effects of six factors on photosynthetic parameters as well as carbon fluxes varied across phenological periods. For example, the correlation between LAI and P_{max} were significant negative in certain periods (e.g., FG_{ON}, LS_{ON}; Figures 7A, B), but were significant positive in off-years (Figure 7H). On the one hand, it

suggested that the greater LAI represents stronger photosynthesis in Moso bamboo forests (Lin et al., 2022; You et al., 2022). On the other hand, the negative direct relationship may be caused by the uncertainties of large-scale remote sense monitoring capture changes at the site scale (Tian et al., 2002) when a rapid leaf spreading during FG_{ON} period. Moreover, the single-peaked shape of LAI time series differs with the bimodal of P_{max} in on-years (Figure 3) also indicate that there may have a certain delay of MODIS LAI product at site scale implementation (Heiskanen et al., 2012), despite we have applied particle filter algorithm to improve its accuracy. Therefore, analyzing the abiotic response mechanisms of carbon fluxes in Moso bamboo forests in the full phenological cycle is particularly important (Song et al., 2017; Chen et al., 2018; Zhou et al., 2019).

4.3 Uncertainty analysis

In this study, we used EddyPro to process 10 Hz of raw flux data to a 30-min time scale and then culled and interpolated it to form a complete flux time series based on standard FLUXNET and ChinaFLUX processing methods, although the processing was subject to some uncertainties (Kim et al., 2020; Zhu et al., 2022). On the one hand, the choice of friction velocity threshold is among the most important causes of uncertainty in rejecting anomalous data from carbon flux observations (Pastorello et al., 2020). Its value generally varies with forest type, and the observed stand conditions of the friction velocity threshold are inconsistent, generally ranging from 0.2 to 0.35 $m \cdot s^{-1}$ (Xu et al., 2016a; Liu et al., 2018; Zhou et al., 2019). Therefore, we adopted 0.2 $m \cdot s^{-1}$ as the threshold based on the variation characteristics of the observed data with some scientific basis. On the other hand, mean diurnal variation method is among the common data interpolation methods (Moffat et al., 2007). However, interpolation of long-missing observations increases the uncertainty of the results due to changes in environmental factors (Richardson et al., 2007). In addition to the mean diurnal variation method, look-up table and ANNs have been relatively hot during the recent years (Mahabhati et al., 2021). However, on the one hand, the performance of look-up table in gap-filling of extralong gaps is not well known (Kim et al., 2020), on the other hand, despite their reliable performance, ANNs – and generally all other machine learning algorithms – face some challenges. Over-fitting, for instance, is a big concern and can happen when the number of degrees of freedom is high, while the training window is not long enough or the quality of the training dataset is low (Zhu et al., 2022). In the present study, although mean diurnal variation method was used, we interpolated day- and nighttime data separately, and flexibly set the fitting window according to meteorological conditions (Xu et al., 2016a), improving data accuracy to some extent.

Carbon fluxes in forest ecosystems of different types and regions does not respond uniformly to biotic and abiotic factors (Baldocchi et al., 2018; Zhao et al., 2022). For example, precipitation is the main driver of carbon flux in African ecosystems (Merbold et al., 2009), whereas the NEP of Dahurian larch forest ecosystems in northeast China is mainly dominated by VPD (Wang et al., 2008). Moreover,

three Canadian boreal black spruce forests differed in their patterns of response to light and temperature (Bergeron et al., 2007). For Moso bamboo forest ecosystems, previous studies indicated that Ta is the most influential factor of RE on a monthly scale, and PAR, Ts, and VPD influence NEE the most (Liu et al., 2018; Chen et al., 2019). Therefore, although all common biotic and abiotic factors were not included in the current study, the selected factors were those significantly affecting carbon fluxes in Moso bamboo forest ecosystems, giving reliable results.

Pathway modeling is crucial in solving the PCs, and different models can lead to different results (Klem, 1995). For example, Wetzels et al. (2009) discussed the different between SEM and PLS pathways, and Papin et al. (2004) examined the differences in the results of path analysis conducted using basic and extreme pathways. In the present study, the overall pathway frameworks (Figure 2) of “environmental factors - photosynthetic parameter - GEP - NEE” and “environmental factors - RE - NEE” were developed based on the importance of photosynthetic parameters in the carbon cycle (Lin et al., 2022) and the significant influence of environmental factors on respiration (Li et al., 2020). However, time and labor cost constraints led to the insufficient consideration of biotic factors (e.g., chlorophyll fluorescence, LAI, etc.) acquired by remote sensing in this modeling framework, which will be improved in future studies.

5 Conclusion

In this study, based on flux observations and micrometeorological observations using the eddy covariance technique and field observation experiments, we analyzed the changes in carbon fluxes and photosynthetic parameters of Moso bamboo forest ecosystems in the full phenological cycle of 2011–2015. We further analyzed their direct and indirect drivers using correlation and path analyses. The main conclusions were as follows:

1. The photosynthetic capacity of the full phenological cycle was the strongest in LS, with an average P_{max} of 0.75 and 0.68 $mg \cdot m^{-2} \cdot s^{-1}$ for LS_{ON} and LS_{OFF} , respectively. NF_{OFF} had the weakest photosynthetic capacity, with an average P_{max} of 0.42 $mg \cdot m^{-2} \cdot s^{-1}$. The carbon sink and photosynthetic capacities of the ecosystem were synchronous, and the top two are LS_{OFF} and LS_{ON} , whose average NEEs were -23.85 and -19.04, respectively. NF_{OFF} showed the weakest capacity with the value of -3.37 $gC \cdot m^{-2}$. Interannually, photosynthetic capacity was higher in on-than in off-years, with a mean P_{max} of 0.63 and 0.57 $mg \cdot m^{-2} \cdot s^{-1}$, respectively, and mean NEE of -1181.14 and -948.27 $gC \cdot m^{-2} \cdot a^{-1}$, respectively.
2. Ts was the most important driver of the effects of abiotic factors on the annual photosynthetic and carbon sequestration capacities of the Moso bamboo forest ecosystems, especially during bamboo forests focused on stem and underground part growth showcasing direct effects on P_{max} (NF_{ON} : -0.62, FG_{ON} : -1.41) and corresponding indirect effects on NEE (NF_{ON} : 0.65, FG_{ON} : 0.88). In contrast, when the focus shifted to leaf

growth, T_a emerged as the main driver, with PCs of T_a concerning P_{max} being -0.91, -0.52, and -1.35 for LR_{OFF} , LS_{ON} , and LS_{OFF} , respectively, and indirect effects on NEE of 0.32, 0.23, and -1.42, respectively.

- The increase in LAI significantly enhanced the net carbon capacity, especially in off-years, exhibiting the highest correlation with NEE was the among the six factors (-0.59). The effect of LAI on P_{max} and NEE had a hysteresis during the six phenological periods when leaves were still growing, and LAI promoted P_{max} when leaf growth was stable in the long period, e.g., its PCs with P_{max} were 0.67, 0.02, and 0.16 in LR_{OFF} , NF_{ON} , and off-years, respectively.

Data availability statement

The original contributions presented in the study are included in the article/Supplementary Material, further inquiries can be directed to the corresponding author/s.

Author contributions

CX: Conceptualization, Data curation, Investigation, Methodology, Software, Writing – original draft, Writing – review & editing. FM: Methodology, Supervision, Writing – review & editing. HD: Methodology, Supervision, Writing – review & editing. XL: Data curation, Supervision, Writing – review & editing. JS: Data curation, Software, Writing – review & editing. FY: Data curation, Software, Writing – review & editing. XT: Data curation, Writing – review & editing. ZZ: Data curation, Writing – review & editing. NY: Data curation, Writing – review & editing.

References

- Baldocchi, D., Chu, H., and Reichstein, M. (2018). Inter-annual variability of net and gross ecosystem carbon fluxes: A review. *Agric. For. Meteorol.* 249, 520–533. doi: 10.1016/j.agrformet.2017.05.015
- Bergeron, O., Margolis, H. A., Black, T. A., Coursolle, C., Dunn, A. L., Barr, A. G., et al. (2007). Comparison of carbon dioxide fluxes over three boreal black spruce forests in Canada. *Glob. Change Biol.* 13, 89–107. doi: 10.1111/j.1365-2486.2006.01281.x
- Chang, X., Xing, Y., Gong, W., Yang, C., Guo, Z., Wang, D., et al. (2023). Evaluating gross primary productivity over 9 ChinaFlux sites based on random forest regression models, remote sensing, and eddy covariance data. *Sci. Total. Environ.* 875, 162601. doi: 10.1016/j.scitotenv.2023.162601
- Chen, L., Liu, Y., Zhou, G., Mao, F., Du, H., Xu, X., et al. (2019). Diurnal and seasonal variations in carbon fluxes in bamboo forests during the growing season in Zhejiang province, China. *J. For. Res.* 30, 657–668. doi: 10.1007/s11676-017-0570-9
- Chen, L., Zhou, G., Du, H., Liu, Y., Mao, F., Xu, X., et al. (2018). Simulation of CO₂ fluxes in Moso bamboo forest based on random forest model and its influence factors. *Sci. Silv. Sin.* 54, 1–12. doi: 10.11707/j.1001-7488.20180801
- Chen, S., Lin, G., Huang, J., and Jenerette, G. D. (2009). Dependence of carbon sequestration on the differential responses of ecosystem photosynthesis and respiration to rain pulses in a semiarid steppe. *Glob. Change Biol.* 15, 2450–2461. doi: 10.1111/j.1365-2486.2009.01879.x
- Chen, X., Jiang, H., Niu, X., Zhang, J., Liu, Y., and Fang, C. (2016). Effects of seasonal heat and drought on carbon fluxes in subtropical Moso bamboo forests. *Chin. J. Appl. Ecol.* 27, 335–344.
- Chu, H., Luo, X., Ouyang, Z., Chan, W. S., Dengel, S., Biraud, S. C., et al. (2021). Representativeness of Eddy-Covariance flux footprints for areas surrounding AmeriFlux sites. *Agric. For. Meteorol.* 301, 108350. doi: 10.1016/j.agrformet.2021.108350
- Du, Y., Wang, Y. P., Su, F., Jiang, J., Wang, C., Yu, M., et al. (2020). The response of soil respiration to precipitation change is asymmetric and differs between grasslands and forests. *Glob. Change Biol.* 26, 6015–6024. doi: 10.1111/gcb.15270
- Falge, E., Baldocchi, D., Olson, R., Anthoni, P., Aubinet, M., Bernhofer, C., et al. (2001). Gap filling strategies for defensible annual sums of net ecosystem exchange. *Agric. For. Meteorol.* 107, 43–69. doi: 10.1016/S0168-1923(00)00225-2
- Fang, Y., Mo, J., Huang, Z., and Ouyang, X. (2003). Carbon accumulation and distribution in Pinus massoniana and Schima superba mixed forest ecosystem in Dinghushan Biosphere Reserve. *J. Trop. Subtrop. Bot.* 11, 47–52. doi: 10.3969/j.issn.1005-3395.2003.1.010
- Flexas, J., and Carriqui, M. (2020). Photosynthesis and photosynthetic efficiencies along the terrestrial plant's phylogeny: lessons for improving crop photosynthesis. *Plant J.* 101, 964–978. doi: 10.1111/tpj.14651
- Friedlingstein, P., O'sullivan, M., Jones, M. W., Andrew, R. M., Gregor, L., Hauck, J., et al. (2022). Global carbon budget 2022. *ESSD Dis.* 2022, 1–159. doi: 10.5194/essd-14-4811-2022
- Ge, X., Cao, Y., Zhou, B., Xiao, W., Tian, X., and Li, M.-H. (2020). Combined application of biochar and N increased temperature sensitivity of soil respiration but still decreased the soil CO₂ emissions in moso bamboo plantations. *Sci. Total. Environ.* 730, 139003. doi: 10.1016/j.scitotenv.2020.139003

Funding

The author(s) declare financial support was received for the research, authorship, and/or publication of this article. The authors gratefully acknowledge the support of Leading Goose Project of Science Technology Department of Zhejiang Province (No. 2023C02035), Scientific Research Project of Baishanzu National Park (No. 2022JBGS02), National Natural Science Foundation of China (No. 32171785, 32201553, 31901310).

Conflict of interest

The authors declare that the research was conducted in the absence of any commercial or financial relationships that could be construed as a potential conflict of interest.

Publisher's note

All claims expressed in this article are solely those of the authors and do not necessarily represent those of their affiliated organizations, or those of the publisher, the editors and the reviewers. Any product that may be evaluated in this article, or claim that may be made by its manufacturer, is not guaranteed or endorsed by the publisher.

Supplementary material

The Supplementary Material for this article can be found online at: <https://www.frontiersin.org/articles/10.3389/fpls.2024.1359265/full#supplementary-material>

- Gitelson, A. A., Gamon, J. A., and Solovchenko, A. (2017). Multiple drivers of seasonal change in PRI: Implications for photosynthesis 2. *Stand level. Remote Sens. Environ.* 190, 198–206. doi: 10.1016/j.rse.2016.12.015
- Gong, Y., Ji, X., Hua, Y., Zhang, Y., and Li, N. (2020). Progress in the study of carbon dioxide fluxes in forest ecosystems based on eddy covariance techniques. *J. Zhejiang A F Univ.* 37, 593–604.
- Gu, D., He, W., Huang, K., Otieno, D., Zhou, C., He, C., et al. (2019). Transpiration of Moso bamboo in southern China is influenced by ramet age, phenology, and drought. *For. Ecol. Manage.* 450, 117526. doi: 10.1016/j.foreco.2019.117526
- Harris, N. L., Gibbs, D. A., Baccini, A., Birdsey, R. A., De Bruin, S., Farina, M., et al. (2021). Global maps of twenty-first century forest carbon fluxes. *Nat. Clim. Change* 11, 234–240. doi: 10.1038/s41558-020-00976-6
- Heiskanen, J., Rautiainen, M., Stenberg, P., Möttöus, M., Vesanto, V.-H., Korhonen, L., et al. (2012). Seasonal variation in MODIS LAI for a boreal forest area in Finland. *Remote Sens. Environ.* 126, 104–115. doi: 10.1016/j.rse.2012.08.001
- Hsu, P.-K., Takahashi, Y., Merilo, E., Costa, A., Zhang, L., Kernig, K., et al. (2021). Raf-like kinases and receptor-like (pseudo) kinase GHR1 are required for stomatal vapor pressure difference response. *Proc. Natl. Acad. Sci.* 118, e2107280118. doi: 10.1073/pnas.2107280118
- Huang, Z., Li, X., Du, H., Zou, W., Zhou, G., Mao, F., et al. (2023). An algorithm of forest age estimation based on the forest disturbance and recovery detection. *IEEE Trans. Geosci. Remote.* 61, 1–18. doi: 10.1109/TGRS.2023.3322163
- Iturbide, M., Gutiérrez, J. M., Alves, L. M., Bedia, J., Cerezo-Mota, R., Cimadevilla, E., et al. (2020). An update of IPCC climate reference regions for subcontinental analysis of climate model data: definition and aggregated datasets. *Earth Syst. Sci. Data* 12, 2959–2970. doi: 10.5194/essd-12-2959-2020
- Jia, X., Mu, Y., Zha, T., Wang, B., Qin, S., and Tian, Y. (2020). Seasonal and interannual variations in ecosystem respiration in relation to temperature, moisture, and productivity in a temperate semi-arid shrubland. *Sci. Total. Environ.* 709, 136210. doi: 10.1016/j.scitotenv.2019.136210
- Jiang, Y., Wang, B., Niu, X., Dong, Z., and Wang, P. (2016). Contribution of soil fauna respiration to CO₂ flux in subtropical Moso bamboo (*Phyllostachys pubescens*) forests: A comparison of different soil treatment methods. *Environ. Earth Sci.* 75, 1–11. doi: 10.1007/s12665-016-5528-2
- Kang, F., Li, X., Du, H., Mao, F., Zhou, G., Xu, Y., et al. (2022). Spatiotemporal evolution of the carbon fluxes from bamboo forests and their response to climate change based on a BEPS model in China. *Remote Sens.* 14, 366. doi: 10.3390/rs14020366
- Kim, Y., Johnson, M. S., Knox, S. H., Black, T. A., Dalmagro, H. J., Kang, M., et al. (2020). Gap-filling approaches for eddy covariance methane fluxes: A comparison of three machine learning algorithms and a traditional method with principal component analysis. *Glob. Change Biol.* 26, 1499–1518. doi: 10.1111/gcb.14845
- Klem, L. (1995). "Path analysis," in *Reading and understanding multivariate statistics* (pp. 65–97). Eds. L. G. Grimm and P. R. Yarnold. American Psychological Association.
- Kondo, M., Saitoh, T. M., Sato, H., and Ichii, K. (2017). Comprehensive synthesis of spatial variability in carbon flux across monsoon Asian forests. *Agric. For. Meteorol.* 232, 623–634. doi: 10.1016/j.agrformet.2016.10.020
- Li, X., Du, H., Mao, F., Zhou, G., Xing, L., Liu, T., et al. (2020). Mapping spatiotemporal decisions for sustainable productivity of bamboo forest land. *Land Degrad. Dev.* 31, 939–958. doi: 10.1002/ldr.3509
- Li, X., Du, H., Zhou, G., Mao, F., Zheng, J., Liu, H., et al. (2021). Spatiotemporal dynamics in assimilated-LAI phenology and its impact on subtropical bamboo forest productivity. *Int. J. App. Earth Observ. Geoinform.* 96, 102267. doi: 10.1016/j.jag.2020.102267
- Li, X., Du, H., Zhou, G., Mao, F., Zhu, D., Zhang, M., et al. (2023). Spatiotemporal patterns of remotely sensed phenology and their response to climate change and topography in subtropical bamboo forests during 2001–2017: a case study in Zhejiang Province, China. *GIScience Remote Sen.* 60, 2163575. doi: 10.1080/15481603.2022.2163575
- Li, L., Li, N., Lu, D., and Chen, Y. (2019). Mapping Moso bamboo forest and its on-year and off-year distribution in a subtropical region using time-series Sentinel-2 and Landsat 8 data. *Remote Sens. Environ.* 231, 111265. doi: 10.1016/j.rse.2019.111265
- Li, X., Mao, F., Du, H., Zhou, G., Xu, X., Han, N., et al. (2017). Assimilating leaf area index of three typical types of subtropical forest in China from MODIS time series data based on the integrated ensemble Kalman filter and PROSAIL model. *ISPRS J. Photogramm. Remote Sens.* 126, 68–78. doi: 10.1016/j.isprsjprs.2017.02.002
- Li, H., Zhang, F., Li, Y., Cao, G., Zhao, L., and Zhao, X. (2014). Seasonal and interannual variations of ecosystem photosynthetic features in an alpine dwarf shrubland on the Qinghai-Tibetan Plateau, China. *Photosynthetica* 52, 321–331. doi: 10.1007/s11099-014-0035-8
- Lin, Y., Chen, Z., Yang, M., Chen, S., Gao, Y., Liu, R., et al. (2022). Temporal and spatial variations of ecosystem photosynthetic parameters in arid and semi-arid areas of China and its influencing factors. *Chin. J. Plant Ecol.* 46, 1461–1472. doi: 10.17521/cjpe.2021.0426
- Liu, Y., Zhou, G., Du, H., Berninger, F., Mao, F., Li, X., et al. (2018). Response of carbon uptake to abiotic and biotic drivers in an intensively managed Lei bamboo forest. *J. Environ. Manage.* 223, 713–722. doi: 10.1016/j.jenvman.2018.06.046
- Lloyd, J., and Taylor, J. (1994). On the temperature dependence of soil respiration. *Funct. Ecol.* 8(3), 315–323. doi: 10.2307/2389824
- Luo, Y., and Zhou, X. (2010). *Soil respiration and the environment* (Burlington, USA: Elsevier).
- Mahabhati, A., Beringer, J., Leopold, M., McHugh, I., Cleverly, J., Isaac, P., et al. (2021). A comparison of gap-filling algorithms for eddy covariance fluxes and their drivers. *Geoscientific Instrumentation Methods Data Syst.* 10, 123–140. doi: 10.5194/gi-10-123-2021
- Mao, F., Du, H., Zhou, G., Li, X., Xu, X., Li, P., et al. (2017a). Coupled LAI assimilation and BEPS model for analyzing the spatiotemporal pattern and heterogeneity of carbon fluxes of the bamboo forest in Zhejiang Province, China. *Agric. For. Meteorol.* 242, 96–108. doi: 10.1016/j.agrformet.2017.03.022
- Mao, F., Du, H., Zhou, G., Zheng, J., Li, X., Xu, Y., et al. (2022). Simulated net ecosystem productivity of subtropical forests and its response to climate change in Zhejiang Province, China. *Sci. Total. Environ.* 838, 155993. doi: 10.1016/j.scitotenv.2022.155993
- Mao, F., Li, P., Zhou, G., Du, H., Xu, X., Shi, Y., et al. (2016). Development of the BIOME-BGC model for the simulation of managed Moso bamboo forest ecosystems. *J. Environ. Manage.* 172, 29–39. doi: 10.1016/j.jenvman.2015.12.013
- Mao, F., Zhou, G., Li, P., Du, H., Xu, X., Shi, Y., et al. (2017b). Optimizing selective cutting strategies for maximum carbon stocks and yield of Moso bamboo forest using BIOME-BGC model. *J. Environ. Manage.* 191, 126–135. doi: 10.1016/j.jenvman.2017.01.016
- Mei, T., Liu, X., Fang, D., Zhou, G., Ye, C., Li, P., et al. (2020). Spring leafing phenology favors younger culms of moso bamboo: Aspects from water use relations. *Front. Plant Sci.* 11, 550. doi: 10.3389/fpls.2020.00550
- Merbold, L., Ardö, J., Arneth, A., Scholes, R. J., Nouvellon, Y., De Grandcourt, A., et al. (2009). Precipitation as driver of carbon fluxes in 11 African ecosystems. *Biogeosciences* 6, 1027–1041. doi: 10.5194/bg-6-1027-2009
- Moffat, A. M., Papale, D., Reichstein, M., Hollinger, D. Y., Richardson, A. D., Barr, A. G., et al. (2007). Comprehensive comparison of gap-filling techniques for eddy covariance net carbon fluxes. *Agric. For. Meteorol.* 147, 209–232. doi: 10.1016/j.agrformet.2007.08.011
- Oikawa, P., Sturtevant, C., Knox, S., Verfaillie, J., Huang, Y., and Baldocchi, D. (2017). Revisiting the partitioning of net ecosystem exchange of CO₂ into photosynthesis and respiration with simultaneous flux measurements of ¹³CO₂ and CO₂, soil respiration and a biophysical model, CANVEG. *Agric. For. Meteorol.* 234, 149–163. doi: 10.1016/j.agrformet.2016.12.016
- Papin, J. A., Stelling, J., Price, N. D., Klamt, S., Schuster, S., and Palsson, B. O. (2004). Comparison of network-based pathway analysis methods. *Trends Biotechnol.* 22, 400–405. doi: 10.1016/j.tibtech.2004.06.010
- Pastorello, G., Trotta, C., Canfora, E., Chu, H., Christianson, D., Cheah, Y.-W., et al. (2020). The FLUXNET2015 dataset and the ONEFlux processing pipeline for eddy covariance data. *Sci. DATA* 7, 1–27. doi: 10.1038/s41597-020-0534-3
- Richardson, A. D., Andy Black, T., Ciais, P., Delbart, N., Friedl, M. A., Gobron, N., et al. (2010). Influence of spring and autumn phenological transitions on forest ecosystem productivity. *Philos. Trans. R. Soc. B: Biol. Sci.* 365, 3227–3246. doi: 10.1098/rstb.2010.0102
- Richardson, A. D., Hollinger, D. Y. J. A., and Meteorology, F. (2007). A method to estimate the additional uncertainty in gap-filled NEE resulting from long gaps in the CO₂ flux record. *Agric. For. Meteorol.* 147, 199–208. doi: 10.1016/j.agrformet.2007.06.004
- Savitzky, A., and Golay, M. J. (1964). Smoothing and differentiation of data by simplified least squares procedures. *Analytical Chem.* 36, 1627–1639. doi: 10.1021/ac60214a047
- Song, X., Chen, X., Zhou, G., Jiang, H., and Peng, C. (2017). Observed high and persistent carbon uptake by Moso bamboo forests and its response to environmental drivers. *Agric. For. Meteorol.* 247, 467–475. doi: 10.1016/j.agrformet.2017.09.001
- Song, X., Peng, C., Ciais, P., Li, Q., Xiang, W., Xiao, W., et al. (2020). Nitrogen addition increased CO₂ uptake more than non-CO₂ greenhouse gases emissions in a Moso bamboo forest. *Sci. Adv.* 6, eaaw5790. doi: 10.1126/sciadv.aaw5790
- Song, X., Peng, C., Zhou, G., Gu, H., Li, Q., and Zhang, C. (2016). Dynamic allocation and transfer of non-structural carbohydrates, a possible mechanism for the explosive growth of Moso bamboo (*Phyllostachys heterocycla*). *Sci. Rep.-UK* 6, 25908. doi: 10.1038/srep25908
- Tang, X., Fan, S., Qi, L., Guan, F., Cai, C., and Du, M. (2015). Soil respiration and carbon balance in a Moso bamboo (*Phyllostachys heterocycla* (Carr.) Mitford cv. *Pubescens*) forest in subtropical China. *IForest-Biogeosci. Forestry* 8, 606. doi: 10.3832/for1360-007
- Tian, Y., Woodcock, C. E., Wang, Y., Privette, J. L., Shabanov, N. V., Zhou, L., et al. (2002). Multiscale analysis and validation of the MODIS LAI product: I. *Uncertain. assess. Remote Sens. Environ.* 83, 414–430. doi: 10.1016/S0034-4257(02)00047-0
- Wang, M., Mori, S., Kurosawa, Y., Ferrio, J. P., Yamaji, K., and Koyama, K. (2021). Consistent scaling of whole-shoot respiration between Moso bamboo (*Phyllostachys pubescens*) and trees. *J. Plant Res.* 134, 989–997. doi: 10.1007/s10265-021-01320-5
- Wang, H.-m., Saigusa, N., Zu, Y.-g., Wang, W.-j., Yamamoto, S., and Kondo, H. (2008). Carbon fluxes and their response to environmental variables in a Dahurian

- larch forest ecosystem in northeast China. *J. For. Res.* 19, 1–10. doi: 10.1007/s11676-008-0001-z
- Wetzels, M., Odekerken-Schröder, G., and Van Oppen, C. (2009). *Using PLS path modeling for assessing hierarchical construct models: Guidelines and empirical illustration* (MIS quarterly: 177-195).
- Xie, J., Chen, J., Sun, G., Chu, H., Noormets, A., Ouyang, Z., et al. (2014). Long-term variability and environmental control of the carbon cycle in an oak-dominated temperate forest. *For. Ecol. Manage.* 313, 319–328. doi: 10.1016/j.foreco.2013.10.032
- Xu, X., Du, H., Zhou, G., Li, P., Shi, Y., and Zhou, Y. (2016a). Eddy covariance analysis of the implications of drought on the carbon fluxes of Moso bamboo forest in southeastern China. *Trees* 30, 1807–1820. doi: 10.1007/s00468-016-1414-5
- Xu, Y., Li, X., Du, H., Mao, F., Zhou, G., Huang, Z., et al. (2023). Improving extraction phenology accuracy using SIF coupled with the vegetation index and mapping the spatiotemporal pattern of bamboo forest phenology. *Remote Sens. Environ.* 297, 113785. doi: 10.1016/j.rse.2023.113785
- Xu, X., Zhou, G., Du, H., Sun, S., and Gao, G. (2016b). Interannual variation of total primary productivity of Moso bamboo forest and its driving factors - A case study of Anji County. *Acta Ecol. Sin.* 36, 1636–1644. doi: 10.5846/stxb201408081584
- Yan, M., Mao, F., Du, H., Li, X., Chen, Q., Ni, C., et al. (2023). Spatiotemporal dynamic of subtropical forest carbon storage and its resistance and resilience to drought in China. *Front. Plant Sci.* 14, 1067552. doi: 10.3389/fpls.2023.1067552
- You, C., Wang, Y., Tan, X., Zhang, B., Ren, T., Chen, B., et al. (2022). Seasonal and interannual variations of ecosystem photosynthetic characteristics in a semi-arid grassland of Northern China. *J. Plant Ecol.* 15, 961–976. doi: 10.1093/jpe/rtac065
- Yu, G., Chen, Z., Piao, S., Peng, C., Ciais, P., Wang, Q., et al. (2014). High carbon dioxide uptake by subtropical forest ecosystems in the East Asian monsoon region. *Proc. Natl. Acad. Sci.* 111, 4910–4915. doi: 10.1073/pnas.1317065111
- Zhang, L., Wen, G., Wang, S., and Liu, Z. (2011). Analysis of the applicability of a light response model for Moso bamboo. *J. Zhejiang A F Univ.* 28, 187–193.
- Zhang, L., Yu, G., Sun, X., Wen, X., Ren, C., Fu, Y., et al. (2006). Seasonal variations of ecosystem apparent quantum yield (α) and maximum photosynthesis rate (P_{max}) of different forest ecosystems in China. *Agric. For. Meteorol.* 137, 176–187. doi: 10.1016/j.agrformet.2006.02.006
- Zhao, J., Liu, D., Cao, Y., Zhang, L., Peng, H., Wang, K., et al. (2022). An integrated remote sensing and model approach for assessing forest carbon fluxes in China. *Sci. Total. Environ.* 811, 152480. doi: 10.1016/j.scitotenv.2021.152480
- Zheng, Y., Guan, F., Fan, S., Yan, X., and Huang, L. (2022). Dynamics of leaf-litter biomass, nutrient resorption efficiency and decomposition in a moso bamboo forest after strip clearcutting. *Front. Plant Sci.* 12, 799424. doi: 10.3389/fpls.2021.799424
- Zhou, L., Song, Q., Zhang, Y., Fei, X., Deng, Y., Wu, C., et al. (2017). Comparison of light response parameter characteristics of photosynthesis in four forest ecosystems. *Chin. J. Ecol.* 36, 1815–1824.
- Zhou, Y., Zhou, G., Du, H., Shi, Y., Mao, F., Liu, Y., et al. (2019). Biotic and abiotic influences on monthly variation in carbon fluxes in on-year and off-year Moso bamboo forest. *Trees* 33, 153–169. doi: 10.1007/s00468-018-1765-1
- Zhu, S., Clement, R., McCalmont, J., Davies, C. A., and Hill, T. (2022). Stable gap-filling for longer eddy covariance data gaps: A globally validated machine-learning approach for carbon dioxide, water, and energy fluxes. *Agric. For. Meteorol.* 314, 108777. doi: 10.1016/j.agrformet.2021.108777